

SURVEYS FOR PULSED OPTICAL EMISSION FROM RADIO PULSARS

Alberto Carramiñana,¹ Simon Vidrih,^{2,3} and Andrej Čadež^{2,3}

RESUMEN

CLYPOS fue la primera búsqueda sistemática de emisión pulsada en el rango visible en radio pulsares aislados, relacionados con estrellas de neutrones jóvenes aisladas. El censo empleó un estroboscopio acoplado a una cámara espectrógrafo para objetos débiles en un telescopio de 2.12 metros de apertura. Se estudió una muestra de casi 30 pulsares, sin obtener ninguna detección positiva por encima de magnitudes entre 20 y 22. CLYPOS permite acotar la eficiencia en la conversión de energía rotacional en luz visible por debajo de valores entre 10^{-3} y 10^{-7} . Un censo similar en un telescopio de 10 metros de apertura, como el Gran Telescopio Canarias, tendría amplias probabilidades de éxito, permitiendo el estudio de la emisión sincrotrón de los pulsares.

ABSTRACT

CLYPOS was the first survey to search for pulsed optical emission from radio pulsars related to young isolated neutron stars. This survey was performed using a stroboscope device coupled to a FOSC on a 2.12 meter telescope. A sample of nearly 30 pulsars was surveyed with no detections of optical pulses down to magnitudes between 20 and 22. This allows to constraint the values for the efficiency to convert rotational energy into visible light between 10^{-3} and 10^{-7} . A similar survey on a 10-meter class telescope, like the Gran Telescopio Canarias, would be extremely more sensitive and highly likely to result in positive detections, allowing ground-based studies the synchrotron spectra of pulsars.

Key Words: PULSARS — STARS: NEUTRON — SURVEYS

1. PULSARS

Pulsars are universally accepted to be rapidly rotating neutron stars. Magnetic braking provides the energy input for accelerating charged particles and emit electromagnetic and gravitational radiation. This established principle allows to write the energy (E) loss equation

$$\dot{E} = I\Omega\dot{\Omega} = -\frac{2\mu_*^2\Omega^4}{3c^3}, \quad (1)$$

where Ω is the rotational angular frequency, μ is the magnetic dipole moment of the star and I its moment of inertia. Particle acceleration is evident in plerionic environment, as those of the Vela and Crab nebulas, the latter observed jointly by the *Chandra* and *Hubble* Space Telescopes (Weisskopf et al. 2000). A fraction to the energy injected to these particles is radiated within the light cylinder of the neutron star, producing pulsed emission observed in several decades of the electromagnetic spectrum. At least two components have been theoretically inferred in young isolated pulsars: the direct synchrotron emis-

sion from high energy electrons trapped in the strong magnetic field in the vicinity of the star produces radiation with energies ranging from 1 eV (IR/optical) to a few MeV (low-energy gamma-rays); the curvature component is due to the curved path of the same electrons as they move along closed magnetic field lines, producing photons with energies up to a few GeV. Apart from the issue of where does the e^\pm acceleration take place, distinguishing between polar cap and outer gap pulsar models, the luminosity, spectrum and (probably) beaming depends on the physical properties of the neutron star, namely Ω , μ and their relative orientation, $\sin\theta = \hat{\mu} \cdot \hat{\Omega}$.

The optical pulsed emission is the only of the synchrotron and curvature components observable from ground. However, as far as we know, the Crab is the only bright pulsar in the optical, with other detected pulsars typically fainter than the 22 magnitude. The inferred optical efficiencies are low, even for the Crab for which $\eta_{opt} \equiv L_{opt}/\dot{E}_{rot} \sim 10^{-7}$, assuming a beaming angle of 10° . Although one might believe that η_{opt} is likely to decrease with age, a different trend is observed among gamma-ray pulsars, where the *observed* efficiency increases with dynamical age as $\tau^{0.8}$ (Figure 1). This might reflect either an actual increase in the γ -ray efficiency or a narrowing of the emission cone.

¹Instituto Nacional de Astrofísica, Óptica y Electrónica, Tonantzintla, Puebla, México.

²University of Ljubljana, Slovenia.

³Visiting Astronomer, Observatorio Astrofísico Guillermo Haro, Cananea, Sonora, México.

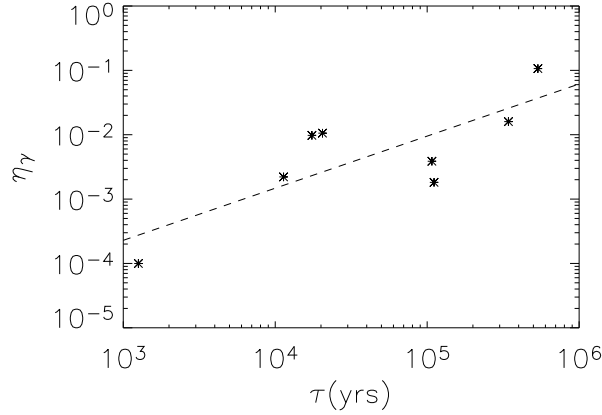


Fig. 1. Efficiency of γ -ray emission as function of characteristic age $\tau = \Omega/2\dot{\Omega}$ for the known gamma-ray pulsars. The best fit is $\log \eta_\gamma = 0.81 \log \tau - 6.07$.

Assuming pulsars have the same efficiency η_{opt} than the Crab, it is possible to compile a list of estimated optical magnitudes for radio pulsars based on their rotational parameters and distance d , inferred from the dispersion measure,

$$m = m_c - 2.5 \log \left\{ \frac{\eta}{\eta_c} \left(\frac{\dot{P}/\dot{P}_c}{P^3/P_c^3} \right) \left(\frac{d}{d_c} \right)^2 \right\}, \quad (2)$$

where the c sub-index indicates the Crab pulsar parameters, taken here as $m_c = 16.5$, $P_c \simeq 33.4$ ms, $\dot{P}_c \simeq 4.21 \times 10^{-13}$ and $d_c = 2$ kpc.

We made a list of 30 young isolated radio pulsars potentially bright in the optical, not reported as detected in this band, and observable from a site at latitude $+30^\circ$. We assumed $\eta = \eta_c$ and neglected the effect of absorption. These objects were the target of the Cananea Ljubljana Young Pulsar Optical Survey.

2. CLYPOS

The Cananea Ljubljana Young Pulsar Optical Survey (CLYPOS) aim was to search for *pulsed* optical emission from radio pulsars using a stroboscopic device adapted to the LFOSC instrument at the 2.12 meter telescope of the Observatorio Astrofísico Guillermo Haro (OAGH) in Cananea, Sonora. Observations of the objects included in Table 1 were made between December 1998 and November 2000. The results of this survey will be presented and discussed in more detail in (Vidrih, Carramiñana, & Čadež 2004).

The stroboscope is basically a rotating chopper wheel with four 9° angular openings, acting as a periodic shutter by obstructing the passage of light 90% of the time in a controlled manner. The chopper can

TABLE 1
THE CLYPOS SAMPLE.

PSR J	P (s)	$\log(\dot{P})$	$\log(\dot{E})$ (erg/s)	d (kpc)	V_{opt}^a mag.
0056 + 4756	0.472	-14.45	33.13	1.00	27.0
0108 - 1431	0.808	-16.09	30.79	0.10	27.8
0117 + 5914	0.101	-14.23	35.34	2.14	23.1
0139 + 5814	0.272	-13.97	34.32	2.89	26.8
0157 + 6212	2.352	-12.72	32.76	1.39	28.9
0358 + 5413	0.156	-14.36	34.66	2.07	24.8
0454 + 5543	0.341	-14.63	33.37	0.79	25.9
0538 + 2817	0.143	-14.44	34.69	1.77	24.3
0543 + 2329	0.246	-13.81	34.61	3.54	26.0
0614 + 2229	0.335	-13.22	34.80	4.72	26.2
0631 + 1036	0.288	-12.98	35.24	6.56	25.8
0659 + 1414	0.385	-13.26	34.58	0.76	22.8
0742 - 2822	0.167	-13.77	35.16	1.89	23.3
0826 + 2637	0.531	-14.77	32.65	0.38	26.1
0908 - 1739	0.402	-15.17	32.61	0.63	27.3
0922 + 0638	0.431	-13.86	33.83	2.97	27.6
0953 + 0755	0.253	-15.64	32.75	0.12	23.3
1136 + 1551	1.188	-14.43	31.94	0.27	27.1
1705 - 1906	0.299	-14.38	33.79	1.18	25.7
1753 - 2502	0.528	-13.85	33.58	0.10	30.9
1825 - 0935	0.769	-13.28	33.66	1.01	25.7
1833 - 0827	0.085	-14.04	35.77	5.67	24.2
1908 + 0734	0.212	-15.08	33.53	0.58	28.6
1932 + 1059	0.227	-14.94	33.59	0.17	22.0
1932 + 2220	0.144	-13.24	35.88	9.80	25.1
2043 + 2740	0.096	-14.90	34.75	1.13	23.2
2337 + 6151	0.495	-12.72	34.79	2.47	24.8

^aOptical magnitudes assume the Crab efficiency and the 1.8 mag enhancement at the pulse peak due to the stroboscope.

be controlled with high accuracy through suitable electronics coupled with a GPS signal. The beam of light coming from the telescope is let to pass 10% of the time for each rotation period, with the wheel rotation easily controlled to match the pulsar frequency. As the wheel has four openings it actually rotates at 1/4 of the set frequency, relaxing the mechanical demands on control.

We have devised two practical operating modes for the stroboscope: phase-locked and phase-drifting. In *phase-locked* mode the system is run at exactly the observed (epoch calculated and barycenter corrected) frequency of the pulsar, keeping the relative phase between the stroboscope and pulsar

fixed during the observations. This allows for images or spectra to be obtained at a fixed pulse phases, as done priorly with the Crab pulsar (Carramiñana, Čadež, & Zwitter 2000). For this pulsar synchronizing the system with the main emission peak enhances the signal of the pulsar 1.8 magnitudes with respect to the background and other objects in the field. The accuracy required in the control of the frequency of the system is about $\Delta\nu/\nu \geq 10^{-8}$ for an 8 hour run on the Crab, reachable with the available set-up. For the purpose of this survey, we found necessary to scan through the different pulse phases. The way we devised to do this was to set the frequency of the stroboscope system to a slightly different value to the pulsar frequency. The value of the frequency offset determines the time needed for a complete scan through the pulse and can be set by the observed. We defined running the chopper wheel with a predetermined constant frequency offset the *phase-drifting mode*.

Synchronizing the stroboscope in absolute phase with the pulsar is a different and more challenging task, as it requires measuring the angular position of the blade at a fixed moment in time. For example, fixing the absolute phase with 1% in a Crab observation requires measuring the angular position of the blade with a precision better than 50 arcmin at a time defined better than 0.3 ms. Our system has recently been upgraded to achieve absolute phase precision (Vidrih 2003), but not by the time of the CLYPOS observations. Control of the absolute phase could be used for future surveys, although in practise most of the pulsars observed through the electromagnetic spectrum do not keep the same absolute phase through all regimes. As a consequence, we believe necessary to scan through pulse phases for a survey targeted to pulsed optical emission.

The stroboscopic system was placed in the trajectory of the beam of light to reach the Landessternwarte Faint Object Spectrograph Camera (LFOSC) of the 2.12 meter telescope of the OAGH. LFOSC uses a focal reducer to allow spectroscopy and photometry (BVRIH α and white light) on a 10×6 arcmin field of view. The LFOSC CCD detector matches 1 arcsec/pixel angular sampling and has a readout time close to 13 seconds. We performed our observations in phase-drift mode, taking a sequence of 24 consecutive images of 5 minutes each for every target. The frequency offset was chosen such as to complete one pulse phase cycle every 8 images (that is 40 minutes plus the accumulated readout time), the whole set of images corresponding to 3 pulse cycles. This gives us the flexibility to test the data

both for a non-pulsed signal, adding all 24 images, or for a pulsed signal, comparing the 8 sets of 3 images corresponding each to a $\Delta\phi \gtrsim 1/8$ pulse phase interval. In order to provide confidence to any potential positive detection, we required any pulsed signal to re-appear on all 3 images corresponding to a same pulse phase interval.

Images were taken without filter, to maximize the S/N ratio. After each cycle of 24 images we took a V image of the whole field, which could be used for an approximate estimate of the V magnitudes of the field through a comparison of white light and V images of photometric standard star fields taken on the same night. We found the white light fluxes to be consistent with V magnitudes within ± 0.5 magnitudes. Using these calibration images we can quantify our results. We did not detect any of the radio pulsars of the sample within limiting magnitudes between $V = 20$ and $V = 22$, depending on the observing conditions for each field, in particular the PSF of the set of images. These limits are not stringent in the sense that none of the pulsars of our sample emitting in the optical with the same efficiency as the Crab would have been detected. However, we can revert the argumentation and give the results as upper limits of the optical efficiency, as show in Figure 2. This constrains the possible values for η between 10^{-3} and 2×10^{-7} . Accounting for the Crab pulsar, this result restricts any power-law dependent increase of efficiency with age to have a power-law index $d \log \eta_{opt}/d \log \tau \lesssim 0.4$. The GeV emission observed by EGRET is due to the curvature component emitted by the high energy electrons, while the optical emission is the synchrotron component of the low-energy electrons. If the γ -ray efficiency increases

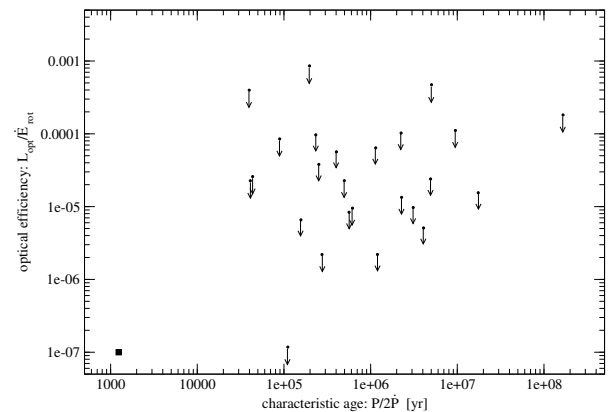


Fig. 2. Upper limits for the efficiency as function of characteristic age $\tau = \dot{\Omega}/2\Omega$ obtained in CLYPOS.

with age while the optical efficiency does not, the electron distribution must harden with time.

3. PULSAR SURVEYS ON LARGE APERTURE TELESCOPES

The principal limitation of the CLYPOS survey was the telescope aperture. The use of a 10-meter telescope on a dark site with good seeing would almost certainly put some of the observed pulsars within reach, as supported by detections of very faint optical counterparts of pulsars using 6-8 meter telescopes and *HST* (Shearer et al. 1997; Zharikov et al. 2002; Mignami, Caraveo, & Bignami 1997).

We note the difficulties of coupling a stroboscopic device to the GTC cameras. For this reason charge shuffling techniques are usually considered for pulsar studies using CCDs. We note that in fact, when the pulsar frequency is known, a stroboscope is probably the most efficient device in terms of signal-to-noise ratio, as it allows arbitrarily long integrations on any phase region of the pulse, adding all the signal inside a PSF area. On the other hand, charge transfer techniques distribute the pulsed signal in several pixels, usually a broad line of width given by the observed PSF (instrumental + seeing).

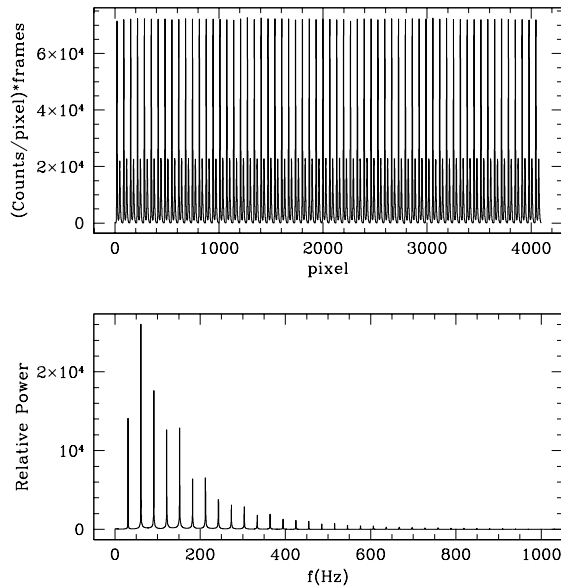


Fig. 3. *upper panel*: simulated integrated counts along the transfer axis of the ELMER CCD for a 10 second integration of the Crab pulsar. *Lower panel*: Fourier transform of the signal above, showing spikes at the 30 Hz input frequency and several harmonics. The strength of the second harmonic indicates the two component nature of the Crab pulse.

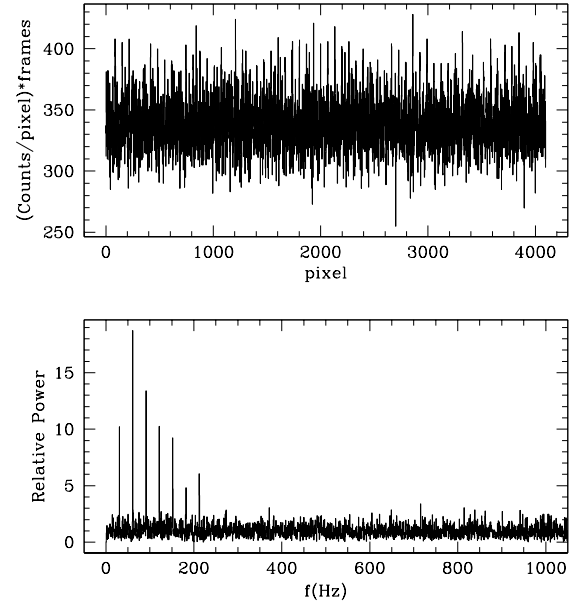


Fig. 4. *upper panel*: simulated integrated counts along the transfer axis of the ELMER CCD for a 60 second integration on a $m = 26.5$ pulsar with the same light-curve as the Crab pulsar. The pulsed signal is not evident along the CCD. *Lower panel*: Fourier transform of the signal above, clearly showing the spikes at the 30 Hz input frequency and several harmonics.

Still, charge transfer techniques can be useful for pulsar work when a 10-meter aperture is available. The CCD detectors of the ELMER camera need a minimum time between consecutive exposures of 500 ms, with is not practical for pulsar timing. Instead the CCDs have to be run on a charge transfer configuration. The ELMER CCD-scan transfer lines on its 2048×4096 pixels at a maximum rate of 1 line every $500 \mu\text{s}$. A mask of 3 minutes \times 12.8 arcsec will be available for timing purposes, with the charge transfer direction along the short axis. Given the scale of 0.2 arcsec/pixel, charge can be accumulated for 32 ms. The effective phase resolution will be due to the PSF width divided by the transfer rate, i.e. 2.5 ms or about $\Delta\phi \approx 0.08$ for the Crab pulsar with a 1 arcsec FWHM PSF. The system will be optimal for pulsar work if the CCD can be run continuously, accumulating signal at one end, transferring it to the other end and reading it without interruption, as in the free-run mode used by (Fordham et al. 2002). Alternatively, exposures can be added together if the start of integration and frame transfer can be precisely timed, to something like $100 \mu\text{s}$ absolute accuracy.

We simulated pulsar observations under the assumptions of a 8% efficiency for ELMER, no filters

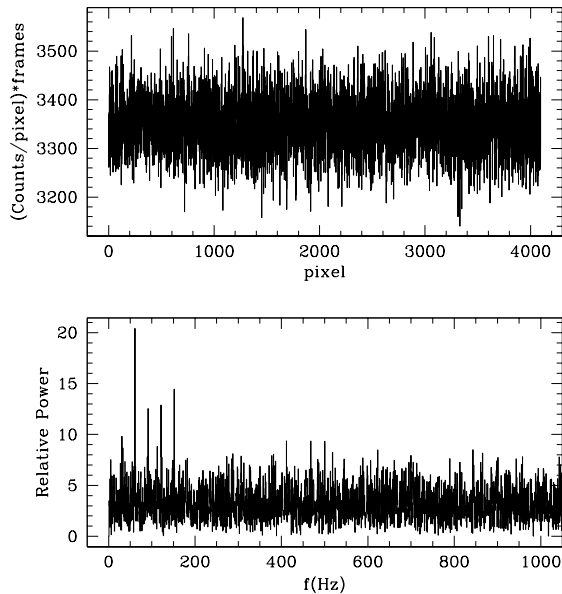


Fig. 5. *upper panel*: simulated integrated counts along the transfer axis of the ELMER CCD for a 600 second integration on a $m = 29.0$ pulsar with the same light-curve as the Crab pulsar. *Lower panel*: Fourier transform of the signal above, showing weak but significant spikes at the 30 Hz input frequency and first few harmonics.

and 1.0 arcsec PSF. As shown in Figure 3 a 10-second exposure on the Crab pulsar gives the clear trace of the periodic signal. This can be Fourier transformed, producing spikes at the pulsar fre-

quency and its harmonics. Either through direct phase-folding of the CCD signal or through the Fourier transforming, the pulsarlight curve can be retrieved. The Crab pulsar is by far the brightest pulsar and spectroscopic studies have been feasible with 2 or 4-meter telescopes (Carramiñana, Čadež, & Zwitter 2000; Fordham et al. 2002). Figure 4 shows a one minute integration on a more challenging 26.5 magnitude pulsar, and Figure 5 shows that even a 29.0 magnitude pulsar might be within the reach of the Gran Telescopio Canarias.

The support of the staff Observatorio Astrofísico Guillermo Haro was essential for the CLYPOS project and is thankfully acknowledged. CLYPOS was supported partially by CONACyT grant 25539-E and the Ministry of Education, Science and Sports of the Republic of Slovenia.

REFERENCES

- Carramiñana, A., Čadež, A., & Zwitter, T. 2000, *ApJ*, 542, 974.
 Fordham, J. L. A, et al. 2002, *ApJ*, 581, 485
 Mignami, R., Caraveo, P. A., & Bignami, G.F. 1997, *ApJ*, 474, L51
 Shearer, A., et al. 1997, *ApJ*, 487, L181
 Vidrih, S., 2003, Ph.D. Thesis, University of Ljubljana
 Vidrih, S., Carramiñana, A., & Čadež, A. 2004, in preparation
 Weisskopf, M.C., et al. 2000, *ApJ*, 536, L81
 Zharikov, S.V., et al. 2002, *A&A*, 393, 505

Andrej Čadež and Simon Vidrih: Faculty of Mathematics and Physics, University of Ljubljana, Jadranska 19, 1000 Ljubljana, Slovenia (simon.vidrih, andrej.cadez@mf.uni-lj.si).

Alberto Carramiñana: Instituto Nacional de Astrofísica, Óptica y Electrónica, Luis Enrique Erro 1, Tonantzintla, Puebla 72840, México (alberto@inaoep.mx).